Landscape Ecol (2015) 30:487–499
DOI 10.1007/s10980-014-0123-y

RESEARCH ARTICLE

Critical loads of nitrogen and sulphur to avert acidification and eutrophication in Europe and China

Maximilian Posch · Lei Duan · Gert Jan Reinds · Yu Zhao

Received: 9 June 2014 / Accepted: 11 November 2014 / Published online: 20 November 2014

Abstract
Introduction Forests and other (semi-)natural ecosystems provide a range of ecosystem services, such as purifying water, stabilizing soils and nutrient cycles, and providing habitats for plants and wildlife. Critical loads are a well-established effects-based approach that has been used for assessing the environmental consequences of air pollution on large regional or national scales.
Materials and methods Typically critical loads of sulphur (S) and nitrogen (N) have been derived separately for characterizing the vulnerability of ecosystems to acidification (by S and N) and eutrophication (by N). In this paper we combine the two approaches and use multiple criteria, such as critical pH and N concentrations in soil solution, to define a single critical load function of N and S.
Results and conclusions The methodology is used to compute and map critical loads of N and S in two regions of comparable size, Europe and China. We also assess the exceedance of those critical loads under globally modelled present and selected future N and S depositions. We also present an analysis, in which the sensitivity of the critical loads and their exceedances to the choice of the chemical criteria is investigated. As pH and N concentration in soil solution are abiotic variables also linked to plant species occurrence, this approach has the potential for deriving critical loads for plant species diversity.

Keywords Critical load function · Exceedance · Nitrogen · Sulphur

M. Posch (✉)
Coordination Centre for Effects (CCE), RIVM, P.O.Box 1, 3720 BA Bilthoven, The Netherlands
e-mail: max.posch@rivm.nl

L. Duan
School of Environment, Tsinghua University, Beijing 100084, People's Republic of China

G. J. Reinds
Alterra, Wageningen University and Research Centre (WUR), P.O.Box 47, 6700 AA Wageningen, The Netherlands

Y. Zhao
School of the Environment, Nanjing University, Nanjing 210023, People's Republic of China

Introduction

Critical loads of S and N have been used as an indicators of ecosystem sensitivity to acidification and eutrophication for more than three decades. Critical loads (or sulphate) were first defined in the mid-1980s for surface waters in Canada (e.g. Jeffries and Lam 1993) and the Nordic countries in Europe (e.g. Henriksen et al. 1992). Under the auspices of the Nordic Council of Ministers and the Convention on Long-range Transboundary Air Pollution (LRTAP) of the United Nations Economic Commission for Europe (UNECE) the critical loads methodology was further developed and extended to terrestrial ecosystems (e.g. Nilsson and Grennfelt 1988), resulting in a periodically

updated manual for the calculation and mapping of critical loads (ICP- Modelling and Mapping 2004). In this context, a critical load is defined as "a quantitative estimate of an exposure to one or more pollutants below which significant harmful effects on specified sensitive elements of the environment do not occur according to present knowledge" (Nilsson and Grennfelt 1988).

Over the last two decades, critical loads have been determined and mapped in several studies for a number of regions: Europe (e.g. De Vries et al. 1994), south-eastern Asia (Hettelingh et al. 1995a), northern Asia (e.g. Bashkin et al. 1995; Reinds et al. 2008), the Arctic region (Forsius et al. 2010), at a global scale (Kuylenstierna et al. 2001; Bouwman et al. 2002) and, for about 15 years, in the P.R. China (Duan et al. 2000; Zhao et al. 2007). In Europe critical loads have been used in integrated assessment (see Reis et al. 2012) to determine cost-effective emission reductions under the UNECE LRTAP Convention (Hettelingh et al. 1995b, 2001, 2007) and, more recently, the air pollution policies of the European Union (Hettelingh et al. 2013). In China, the critical load concept has been applied, e.g., to designate 'acid rain control zones' and 'sulphur dioxide pollution control zones' (Hao et al. 2001), and there are intentions to use it in future policies on multi-pollutant controls (SO_2, NO_x, particulate matter).

In this paper we focus on critical loads for terrestrial ecosystems. Critical loads are either determined empirically or via models. Empirical critical loads are mostly determined for N, are they derived from field experiments or gradient studies that try to establish a link between deposition and damage to the ecosystem. Recent assessments and summaries of empirical critical loads of N as a nutrient can be found in Bobbink and Hettelingh (2011; for Europe) and in Pardo et al. (2011; for the United States). Alternatively, critical loads are derived from biogeochemical soil models, i.e. models that describe the processes in and chemical state of a soil as a function of its properties and driving forces, such as deposition and harvesting. Whereas in 'normal use' models derive the chemical state of the soil as function of the driving forces, critical loads are computed as inverse solutions: given the desired chemical state of the soil, the (maximum) depositions are computed that lead to that state—and these depositions are called critical loads. This task is eased by the fact that critical loads are calculated for a steady state, i.e. transient processes, such as finite buffers (e.g., of base cations) that can delay the impact of depositions, are neglected—the aim being deposition limits that avoid harmful effects in the long run.

Typically, critical loads have been calculated for effects due to acidity (by S and N) and for eutrophying effects by N (Sverdrup and De Vries 1994; Posch and De Vries 1999; De Vries et al. 2003; ICP Modelling and Mapping 2004), using independent chemical criteria relevant for the respective effect. In this paper we combine the two approaches and use multiple criteria, such as critical pH and N concentrations in soil solution, to define a single critical load function of N and S. As pH and N concentration are abiotic variables also linked to plant species occurrence (e.g., Belyazid et al. 2011), this approach has the potential to derive critical loads for criteria related to plant species diversity.

In the following we first derive the critical load function for N and S and then describe the data bases used to calculate critical loads for forests and semi-natural vegetation in Europe and China. We use these data to compute and map critical loads for both regions, and assess the exceedances of those critical loads for different past and future N and S depositions. In a separate section we conduct an analysis by varying the values of the chemical criteria to investigate the sensitivity of the critical loads and their exceedances to the choice of those criteria. We conclude the paper by a discussion of possible generalisations of the critical load function and the uncertainties in critical load calculations.

Methods and materials

Modelled critical loads of N and S

Critical loads are computed with the Simple (or Steady-state) Mass Balance (SMB) model, which links deposition(s) to a chemical variable (the 'chemical criterion') in the soil or soil solution that is associated with undesirable effects (e.g. damage to fine roots) that occur when the 'critical limit' of that criterion is violated. Below we shortly summarise the methods for calculating the critical load of nutrient N (eutrophication) and the critical load of acidity, before combining them into the critical load function of N

and S (for details see ICP- Modelling and Mapping 2004).

The critical load (CL) of nutrient N, $CL_{nut}N$ (e.g. in eq/ha/year), is derived from the steady-state mass balance of N in a single-layer soil compartment as:

$$CL_{nut}N = N_i + N_u + N_{de} + Q[N]_{crit} \quad (1)$$

where N_i, N_u and N_{de} are the long-term average immobilisation in soil, net uptake (i.e. removal by harvest) and denitrification fluxes of N, respectively, Q is the percolating water flux leaving the root zone, and $[N]_{crit}$ is the critical concentration of N, above which the 'harmful effect' occurs. Equation 1 is the simplest form of the critical loads equation, in which all N fluxes are independent from the N deposition. If denitrification is modelled as proportional to the net input of N, i.e. $N_{de} = f_{de}\cdot(N_{dep}–N_i–N_u)$ with a site-specific constant f_{de}, $CL_{nut}N$ is derived as:

$$CL_{nut}N = N_i + N_u + \frac{Q[N]_{crit}}{1 - f_{de}} \quad (2)$$

The critical load of S acidity is derived from the charge balance in soil solution and obtained as:

$$CL_{max}S = BC_{dep} - Cl_{dep} + BC_w - Bc_u - Q[ANC]_{crit} \quad (3)$$

where Bc = Ca + Mg + K and BC = Bc + Na, the indices *dep*, *w* and *u* refer to deposition, weathering and net uptake (i.e. removal by harvest), respectively, and $[ANC]_{crit}$ is the critical concentration of acid neutralising capacity (ANC). $CL_{max}S$ is the maximum deposition of S, S_{dep}, that the ecosystem can stand without causing harm, that is, as long as the N deposition, N_{dep}, is immobilised or taken up, i.e. stays below $CL_{min}N = N_i + N_u$. If $N_{dep} > CL_{min}N$, however, the critical load is a function of both S and N deposition; and for $S_{dep} = 0$ the maximum CL of N is derived as:

$$CL_{max}N = CL_{min}N + CL_{max}S/(1 - f_{de}) \quad (4)$$

The three quantities $CL_{max}S$, $CL_{min}N$ and $CL_{max}N$ define the critical load function of acidifying N and S, depicted in Fig. 1a. For details on the derivation of these equations and their underlying assumptions see ICP- Modelling and Mapping (2004).

The most widely used criteria for avoiding 'harmful effects' of acidity are a critical aluminium (Al) to base cation ratio, a critical Al concentration, or a critical pH (ICP- Modelling and Mapping 2004), as used in this paper. In case of a critical $[H]_{crit} = 10^{-pHcrit}$, the critical ANC leaching can be computed as:

$$[ANC]_{crit} = -[H]_{crit} - K_{gibb}[H]^3_{crit} + \frac{K_1 \cdot DOC}{K_1 + [H]} \quad (5)$$

In Eq. 5 it is assumed that Al-(hydr)oxides are dissolved according to a gibbsite equilibrium; *DOC* is the concentration of dissolved organic acids, the dissociation of which is modelled by assuming them monoprotic with constant K_1 (ICP- Modelling and Mapping 2004). The bicarbonate concentration has been neglected in Eq. 5.

To date, critical loads of acidity and nutrient N have been treated separately. However, in the case of plant diversity, both the availability of N and the acidity status of the soil are of importance. This suggests treating both types of critical loads in conjunction; and the simplest way is to intersect the CL function of acidity with the CL of nutrient N, as illustrated in Fig. 1b. This CL function is characterised by the four quantities $CL_{max}S$, $CL_{min}N$, $CL_{max}N$ and $CL_{nut}N$ in the N–S-deposition plane (dark grey area in Fig. 1b).

It is important to note that a critical load is a (site-specific) ecosystem property, i.e. it does not depend on the depositions of N or S. A critical load is compared to depositions and if—in the simplest case—$ExN = N_{dep}—CL_{nut}N$ is greater than zero for a given N deposition, the critical load of nutrient N is said to be exceeded, and the *ExN* is called the exceedance. For critical load functions, the computation of exceedances becomes more involved: the exceedance is the sum of *ExN* and *ExS*, which are calculated for a given CL function for the different cases of N_{dep} and S_{dep} depositions according to Fig. 2 (for technical details on the calculations see ICP Modelling and Mapping 2004).

To obtain a single exceedance value for a grid cell (for mapping) or an entire region (for tabulation), the average accumulated exceedance, *AAE*, has been defined:

$$AAE = \sum_{j=1}^{n} A_j Ex_j / \sum_{j=1}^{n} A_j \quad (6)$$

where n is the number of ecosystems in the region (grid cell), Ex_j the exceedance of ecosystem j and A_j the area this ecosystem represents; in other words, the AAE is the area-weighted exceedance of the

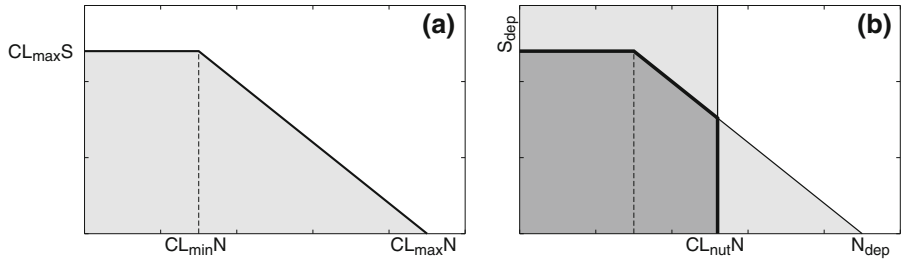

Fig. 1 **a** Critical load function of acidity characterised by the three quantities $CL_{max}S$, $CL_{min}N$ and $CL_{max}N$. The *grey area* indicates N and S depositions for which critical loads are not exceeded; **b** acidity CL function intersected with the critical load of nutrient N, $CL_{nut}N$, defining the N and S CL function. For N and S depositions in the *dark grey area* neither acidity nor nutrient CLs are exceeded; in other words, neither the acidity nor the nutrient N criterion is violated

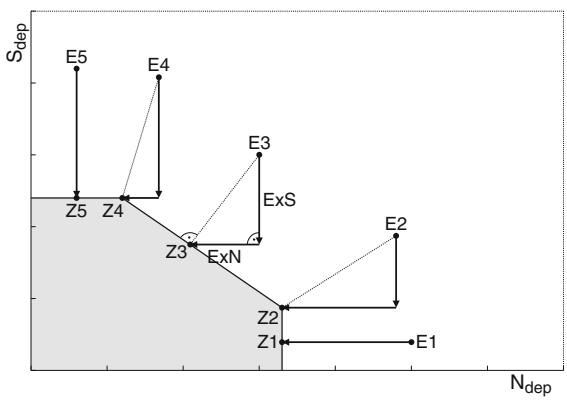

Fig. 2 Illustration of the different cases for calculating the CL exceedance, $Ex = ExN + ExS$, for a given N and S critical load function for different cases of N and S depositions (E1–E5)

individual CLs. To make the AAE a meaningful quantity, Ex_j has to be set to zero in case of non-exceedance (see Posch et al. 2001).

Input data

The required input data for the calculation of critical loads on a regional scale consist of spatial information on climatic variables, base cation deposition and weathering, net nutrient uptake (removal by harvest) and N transformations. In this study critical loads were calculated for forests (EUNIS code 'G'; see Davies et al. 2004) and (semi-)natural vegetation ('D': mires, bogs and fens; 'E': natural grasslands and 'F': heathland, scrub and tundra). In the following the data sources and necessary transformations to obtain those inputs are described separately for Europe and China.

Europe

The European area was restricted to land areas west of 32°E, the area for which the most detailed and complete data sources were available.

(a) *Land cover* We used the European part of the Global Land Cover 2,000 map with 1 km resolution (Bartholome et al. 2002).

(b) *Soils* The European Soil Database v2 map (JRC 2006) at a scale 1:1 M was used for Europe (including Belarus, Ukraine and the European part of Russia). The soil maps are composed of associations, each map polygon representing one soil association. Every association, in turn, consists of several soil typological units (soil types) that each occupy a known percentage of the soil association, but with unknown location within the association. The soil units on the maps are classified into more than 200 soil types (European Soil Bureau Network 2004), with associated attributes such as soil texture, parent material class and drainage class. Six texture classes (including peat) are defined, based on clay and sand content (FAO-UNESCO 2003). Drainage classes were derived from the dominant annual soil water regime.

(c) *Meteorology and hydrology* Long-term (1961–1990) average monthly temperature, precipitation and cloudiness were derived from a high resolution European database (New et al. 1999) that contained monthly values for the years 1901–2001 for land-based grid-cells of $10' \times 10'$ (approx. 15×18 km in central Europe). Evapotranspiration and runoff (precipitation surplus, i.e. water leaving the root

zone) were calculated with a sub-model used in the IMAGE global change model (Leemans and Van den Born 1994), following the approach by Prentice et al. (1993); a description of this model can be found in Reinds et al. (2008). The bottom of the root zone was set at 50 cm, except for lithosols which were assumed to have a soil depth of 10 cm only.

(d) *Base cation deposition and weathering:* Base cation deposition for Europe was taken from simulations with an atmospheric dispersion model for base cations (Van Loon et al. 2005). Weathering of base cations was computed as a function of parent material class and texture class and corrected for temperature, as described in ICP Modelling and Mapping (2004).

(e) *Net growth uptake (removal by harvest), N immobilization and denitrification:* Since CLs describe a steady-state situation, the net growth uptake of base cations and N by forests was computed from the estimated annual average growth of stems and branches and the element contents of Bc and N in these compartments (Jacobsen et al. 2002). Forest growth and harvest data in EU countries was taken from the European Forest Information Scenario (EFISCEN) model (Schelhaas et al. 2007). Forest growth for the rest of Europe was derived from the EFI database (Schelhaas et al. 1999) that provides measured growth data for about 250 regions in Europe for various species and age classes. For the small parts of Russia mapped, forest stock data by Alexeyev et al. (2004) were used; these data were also extrapolated to Belarus and the western part of the Ukraine. For (semi-)natural vegetation no net removal of biomass was assumed, and thus the net uptake was set to zero. The denitrification fraction f_{de}, needed to compute the denitrification flux (see above), was estimated as a function of soil drainage status and varies between 0.1 for well drained soils to 0.8 for peaty soils (ICP Modelling and Mapping 2004). The long-term net N immobilization was set at 1 kg N ha^{-1} $year^{-1}$, which is at the upper end of the estimated annual accumulation rates for the build-up of stable C–N compounds in soils (ICP Modelling and Mapping 2004).

(f) Overlaying these maps and merging polygons with common soil, vegetation and region characteristics within grid cells of 0.05° × 0.05° resulted in about 3.17 million computational units ('sites') with a total area of 2.97 M km^2. The determination of critical loads was limited to units larger than 0.5 km^2, reducing the total number to 1.37 M, covering ~88 % of the study area.

China

(a) *Vegetation* The Chinese Vegetation Map at a scale of 1:2 M was used. The vegetation units on the maps are classified into 95 types (Wu 1980).

(b) *Soils* The Chinese Soil Map at a scale of 1:2 M was used. The soil units on the maps are classified into 43 soil types (Xiong and Li 1987).

(c) *Runoff* The Chinese Runoff Map at a scale of 1:4 M was used (SinoMaps 1984).

(d) *Base cation deposition and weathering:* Atmospheric emissions of Ca and Mg (K and Na are not included due to their negligible shares of base cation emissions) from major anthropogenic sources in China were estimated based on the emission rate and chemical composition of particulate matter (PM). Zhao et al. (2011) estimated that overall emissions were approximately 5.97 and 0.24 Tg $year^{-1}$ for Ca and Mg, respectively, in the year 2005. These estimates were much higher than those for Europe of 0.75–0.80 Tg $year^{-1}$ in 1990 (Lee and Pacyna 1999), highlighting the limits of applying Europe's experience to countries like China, where base cations may have a much larger role in atmospheric chemistry and ecological effects. In addition to the anthropogenic emissions, base cation emissions from wind-blown dust particles from arid and semi-arid regions in northern China were roughly estimated to about 2.08 Tg $year^{-1}$ for Ca and 0.68 Tg $year^{-1}$ for Mg (Zhu et al. 2004). Using a multi-layer, dynamic Eulerian model (Duan et al. 2007; Zhao et al. 2011), the long-range transport and deposition of base cations was estimated. Results show that the total deposition of Ca in China was about

5.29 Tg year^{-1} (with 1.54 Tg year^{-1} as wet deposition and 3.84 Tg year^{-1} as dry deposition), of which anthropogenic sources contributed 67.1 % (92.4 % of wet deposition and 57.6 % of dry deposition). Samples of all major Chinese soil types have been collected in recent years and analysed for physicochemical properties and mineralogy. These data have been used to compute weathering rates of these soil types with the PROFILE model (Duan et al. 2002).

(e) *Nutrient uptake and N immobilization* A literature review on average growth rates and element contents of major plant communities in China was carried out by Duan et al. (2004). Based on this dataset, net uptake rates of N and base cations was estimated for each major vegetation type in China and the results were used in the critical load calculations. N immobilization of major soil groups in China was estimated as the total amount of soil N divided by the period of soil formation (Hao et al. 2003).

(f) *Other parameters* Where needed, these were derived on the basis of ICP- Modelling and Mapping (2004).

Results

Critical loads of N and S

Using the methods and databases described above we calculated the critical load quantities defining the critical load functions of N and S for all sites in Europe and China. Since there are no widely-accepted unique chemical criteria for pH and N, we selected a critical pH of 4.4 (for non-calcareous soils) and a critical N concentration of 1 mg N L^{-1}, independent of location. These values are at the more stringent end of the range of proposed criteria in the literature (Sverdrup and De Vries 1994; Aherne et al. 2001; De Vries et al. 2010). For calcareous soils $CL_{max}S$ was set to 10,000 eq ha^{-1} year^{-1}, reflecting the very high BC weathering rates (and thus pH) in such soils. In this study, those chemical criteria were applied to both Europe and China, leading to a consistent set of critical loads across both regions.

There are many sites and thus critical loads within a single mapping unit (0.5° × 0.5° grid cell), and rather than displaying the mean, we compute the 5-th percentile of the distribution of the critical load values within every grid cell, considering that it is the low critical loads, i.e. the most vulnerable ecosystems, that need attention. In Fig. 3, maps of the 5-th percentiles of the maximum CL of sulphur, $CL_{max}S$, and the CL of nutrient N, $CL_{nut}N$, are displayed. The latter is shown here, since for the chemical criteria chosen $CL_{nut}N < CL_{max}N$ in 99.97 % of the sites. In the exceedance calculations the N and S CL function is used to obtain a single exceedance value (see below).

Very low values of $CL_{max}S$ are found in Sweden and Finland and, to a lesser extent, in the Baltic states; values between 400 and 1,000 eq ha^{-1} year^{-1} are dominant in Germany, Poland and parts of south-eastern Europe as well as in central-western Spain, i.e. in drier areas (small precipitation surplus). High values dominate in the South and on the west coast of Europe, where they are due to the high precipitation—the main reason why Norway and Denmark differ from the Sweden and Finland (Fig. 3a). The generally increasing north–south gradient in $CL_{max}S$ is due to the increasing base cation deposition (and net uptake), which by and large, increase when going south. Critical loads of nutrient N are much lower than the maximum CLs of S (Fig. 3). These values are even more influenced by the runoff, and thus the lowest values correspond strongly with the areas of low precipitation (surplus) in Europe (Fig. 3b); and the highest values are found on the west coast of Europe and the Alps, regions with high precipitation.

Values of $CL_{max}S$ in north-central and north-western China generally exceed 1,500 eq ha^{-1} year^{-1}, attributable mainly to high weathering rates and base cation deposition (Fig. 4a). In the northeast and south, however, the values can be lower than 200 eq ha^{-1} year^{-1}, because of low weathering rates and high base cation uptake. Low $CL_{nut}N$ is commonly found in the northwest, due to very low precipitation and low vegetation N net uptake (Fig. 4b). The values are relatively higher in the south and east, resulting from much higher precipitation and higher soil denitrification rates.

Exceedances

Critical loads provide insight into the spatial distribution of the sensitivity of ecosystems to N and S depositions. To find out whether there is a danger of 'harmful effects', critical loads are compared with present and potential future depositions by calculating

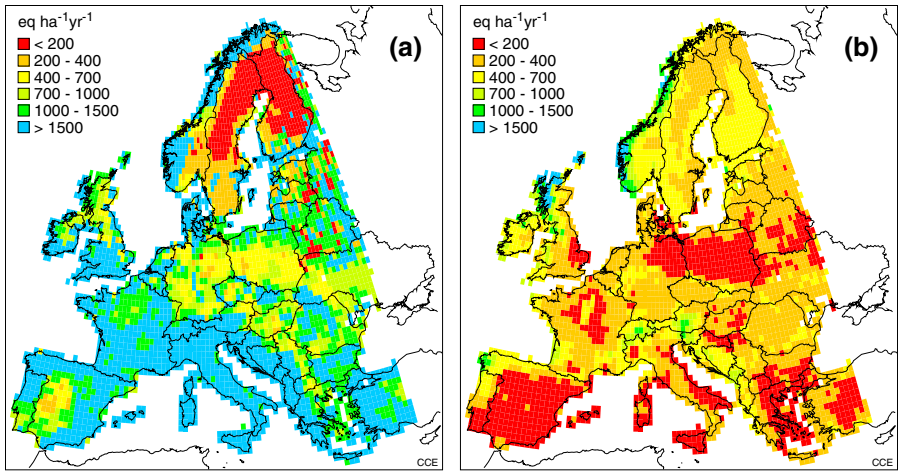

Fig. 3 Gridded (0.5° × 0.5°) 5-th percentile of the critical loads $CL_{max}S$ (*left*) and $CL_{nut}N$ (*right*) for forests and (semi-)natural vegetation in Europe (west of 32°E)

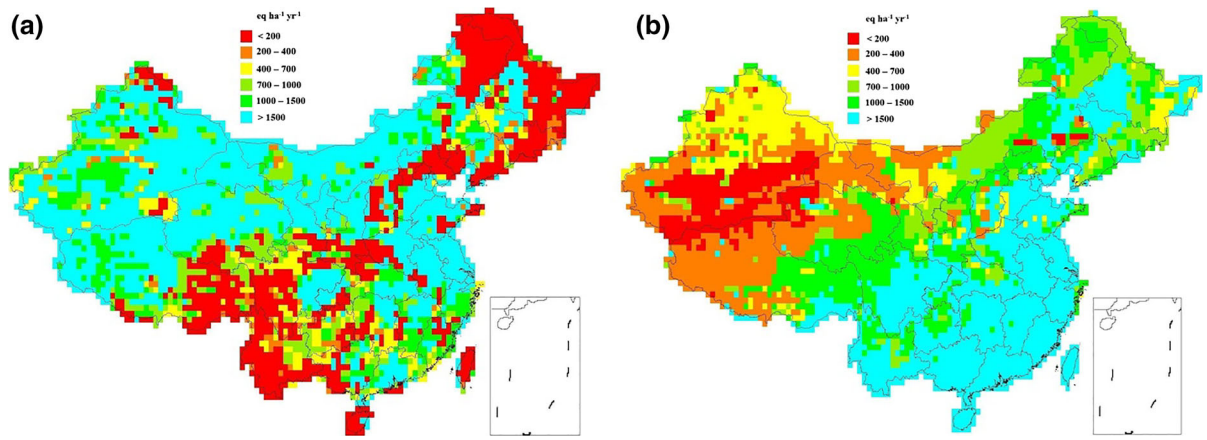

Fig. 4 Gridded 5-th percentile of the critical loads $CL_{max}S$ (*left*) and $CL_{nut}N$ (*right*) in China

the critical load exceedance, i.e. a single number per CL function, as illustrated in Fig. 2. To be able to map exceedances we computed the average accumulated exceedance, *AAE*, as defined in Eq. 6.

As a common and documented basis for exceedance calculations in China and Europe we use S and N depositions available from the Atmospheric Chemistry and Climate Model Intercomparison Project (ACCMIP) (Lamarque et al. 2013). This multi-model deposition dataset provides state-of-the-science, consistent and evaluated gridded (0.5° × 0.5°) global deposition fields (spanning 1850–2100). For the post-2000 atmospheric chemistry, related emissions and concentrations the representative concentration pathways (RCPs) were used (Van Vuuren et al. 2011). These emission pathways ('scenarios') were prepared for the latest assessment of the intergovernmental panel on climate change (IPCC), and thus are more climate-centred rather than looking at N and S emission reduction policies.

Here, in addition to using the 2000 ('present') S and total inorganic N (= $NO_y + NH_x$) depositions, we also computed exceedances with depositions for the year 2100 under the RCP4.5 scenario. The RCP4.5 scenario aims at a stabilization at 4.5 W m^{-2} (~650 ppm CO_2 eq) radiative forcing (see Van Vuuren et al. 2011 for details) and it leads to, by and large, the lowest emissions of S and N in Europe and Asia of the RCP scenario family (see supplementary information of Lamarque et al. 2013). Maps of the

exceedances (AAE) on the 0.5° × 0.5° grid for the years 2000 and 2100 are shown in Fig. 5 (for Europe) and Fig. 6 (for China).

In Europe critical loads in 54.2 % of the ecosystem area are exceeded under the 2000 N and S deposition. Exceedances of critical loads are highest in north-central Europe (Germany, Poland), but also large areas in southern Europe show considerable exceedance. Despite the lowest overall critical loads in Fennoscandia (Fig. 3), large parts are not (or no longer, given that depositions were much higher in the 1970s and 1980s) exceeded, or the exceedance is low. It is interesting to note that computing the exceedances for acidity CLs alone leads to an exceeded area of only 4.7 %, showing that the N-related part of the CL function is much more stringent. Under the RCP4.5 scenario N and S depositions for the year 2100, exceedances decline essentially everywhere in Europe, both in amount (below 700 eq ha^{-1} $year^{-1}$ almost everywhere) and in area (to about 28 %). And a separate calculation shows that the critical loads of acidity would be virtually non-exceeded in all of Europe (exceeded area <0.1 %).

In China, critical loads in about 50 % of the ecosystem area are exceeded under the 2000 N and S deposition (Fig. 6a). Exceedances of critical loads are highest in eastern and south-central China. Those regions have both high S and N depositions, due to the

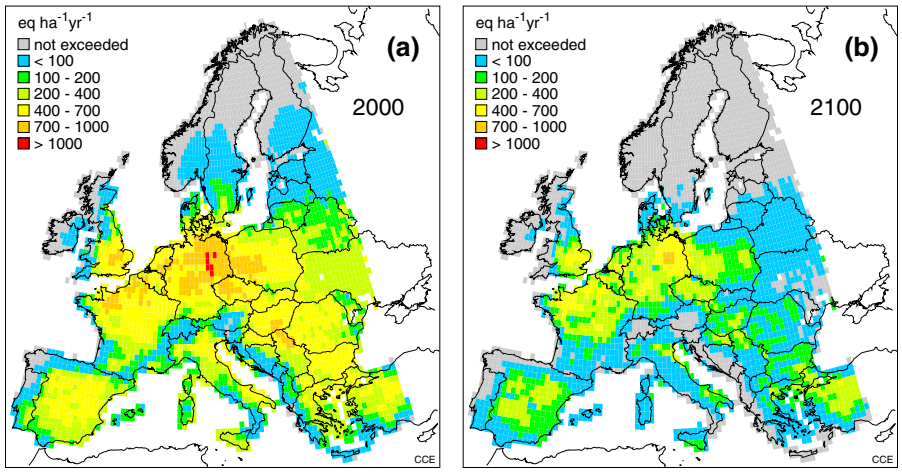

Fig. 5 Exceedance (AAE; see Eq. 6) of critical loads of N and S in Europe in 2000 (*left*) and in 2100 (*right*) under the RCP4.5 scenario

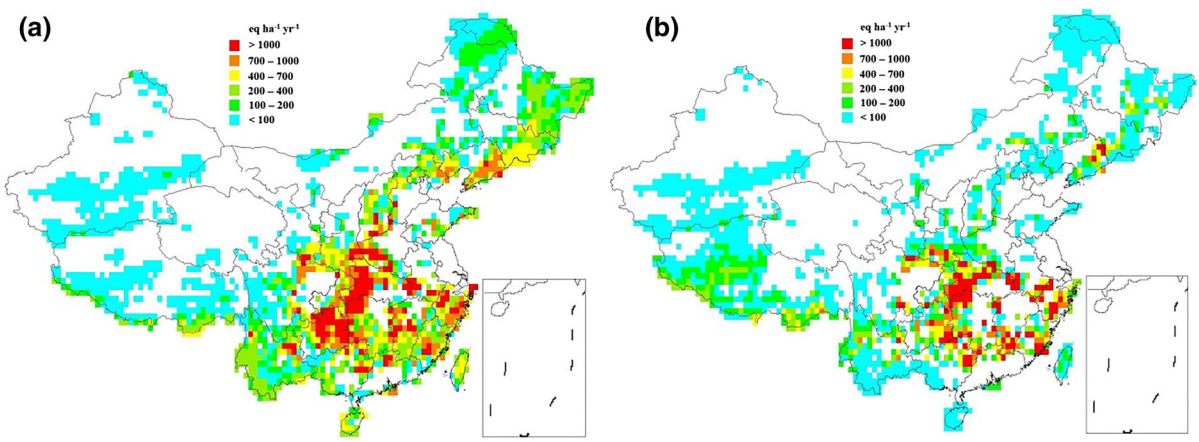

Fig. 6 Exceedance (AAE; see Eq. 6) of critical loads of N and S in China in 2000 (*left*) and in 2100 (*right*) under the RCP4.5 scenario

high density of industry, but mainly S exceedance alone, showing that—in contrast to Europe—the S part of the CL function is much more stringent in these areas. However, the critical load exceedance for almost all regions in western China was due to N deposition; but this exceedance was low. Under the RCP4.5 scenario N and S depositions for the year 2100, exceedances decline somewhat in China, mainly visible in the south-eastern part of the country (Fig. 6b). Since S deposition decreases considerably from 2000 to 2100 but N deposition remains about the same, critical load exceedance in 2100 would be mostly caused by N deposition.

Sensitivity to chemical criteria

The uncertainty and sensitivity in critical load calculations on a large regional scale have been studied before (Reinds et al. 2008, Reinds and De Vries 2010). To investigate the sensitivity of the critical loads and their exceedances on the chemical criteria, we computed the $CL_{max}S$ in Europe also for $pH_{crit} = 4.2$ and 4.6. In Fig. 7a the cumulative distribution functions (cdfs) of the $CL_{max}S$ values for the different pH-criteria are displayed. Surprisingly, for small critical loads (i.e. sensitive ecosystems), the $CL_{max}S$ values do not change much for the different criteria, whereas for high acidity critical loads there is a substantial change in the distributions. An analuguous analysys was carried out for $CL_{nut}N$ and $[N]_{crit}$. Figure 7b shows, in addition to the base case, the cdfs of $CL_{nut}N$ for $[N]_{crit} = 0.5$ and 2.0 mg N L^{-1}. Obviously, there is a considerable influence, but less than the halving or doubling of the critical value might suggest. These graphs show that it is important to carefully select the critical values. However, one has to keep in mind that these are extreme results: in practice it will hardly ever be the case that the uncertaintes in a critical value will all have to be corrected in the same direction.

A similar analysis was carried out for China. As shown in Fig. 8, CLs are much less sensitive to the changes in the criteria in China than in Europe. In contrast to Europe, the $CL_{max}S$ values change more for small values. As in Europe, the bigger change in the distributions occurs for high nutrient N critical loads. Note that, in China there is a considerable area with $CL_{max}S = 0$; this happens in forest areas where the removal (vegetation uptake and leaching) is higher than the input of base cations (weathering and deposition).

A change in critical loads due to a change in criteria (or any other input parameter) is one thing; however, in applications it is of more relevance how exceedances change under different criteria for the CL function. Using the variation in the criteria as above, the cdfs of the resulting exceedances (AAE) in the year 2000 in Europe and China are displayed in Fig. 9. The results are interesting, reflecting the different pollution climates in Europe and China. For Europe, the change in the critical pH hardly matters. This is due to the fact, that S depositions are already quite low in most of Europe, and thus exceedances are driven by N deposition (alone). This is also reflected in the graphs: The changes in the N criterion (halving and doubling of the $[N]_{crit}$) results in a reduction/increase of the non-exceeded area of about 15 % (around a reference value

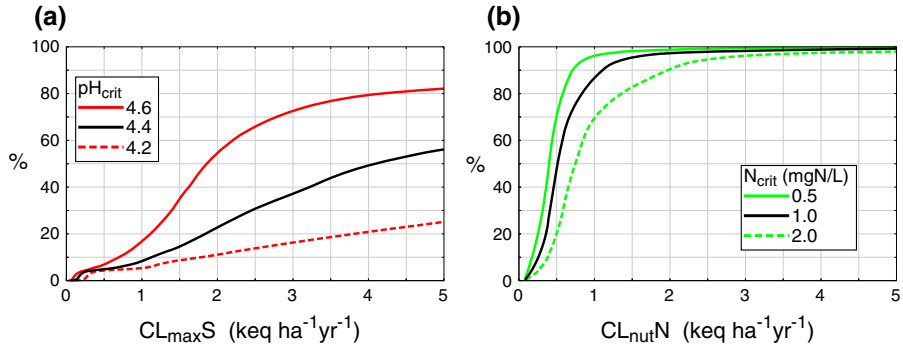

Fig. 7 Cumulative distribution functions (cdfs) of $CL_{max}S$ (**a**) and $CL_{nut}N$ (**b**) in Europe for different critical values. The *black curves* show the base cases ($pH_{crit} = 4.4$, $[N]_{crit} = 1$ mg N L^{-1}), whereas the *red* and *green curves* show the cdfs of $CL_{max}S$ and $CL_{nut}N$, respectively, for the values used in the sensitivity analysis (see legends)

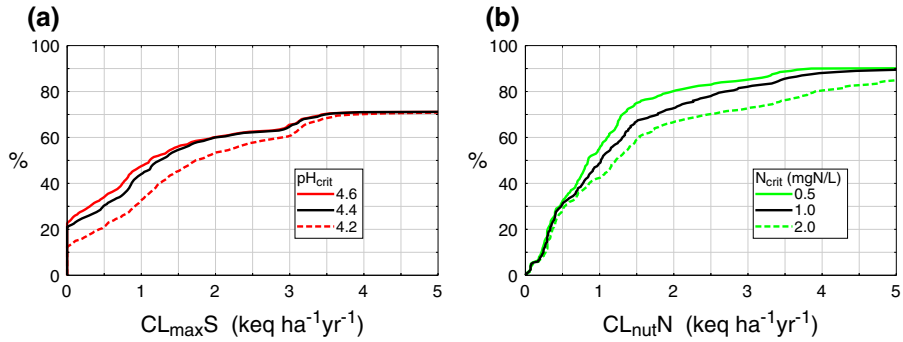

Fig. 8 Cumulative distribution functions (cdfs) of $CL_{max}S$ (**a**) and $CL_{nut}N$ (**b**) in China for different critical values. The *black curves* show the base cases ($pH_{crit} = 4.4$, $[N]_{crit} = 1$ mg N L^{-1}), whereas the *red* and *green curves* show the cdfs of $CL_{max}S$ and $CL_{nut}N$, respectively, for the values used in the sensitivity analysis (see legends)

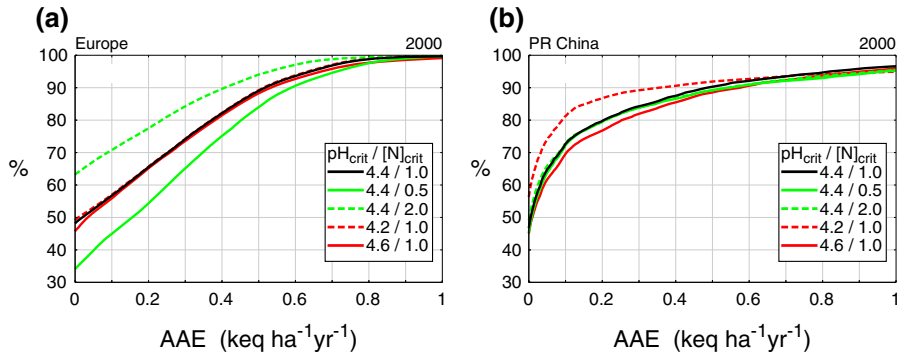

Fig. 9 Cumulative distribution functions of the exceedance (AAE; see Eq. 6) of critical loads in **a** Europe and **b** China in the year 2000 for the different combinations of chemical criteria (pH_{crit} and $[N]_{crit}$). The *black line* represents the base case ($pH_{crit} = 4.4$, $[N]_{crit} = 1$ mg N L^{-1}) and the *coloured lines* correspond to the values shown in Figs. 7 and 8

of 50 %; see intersection of the cdfs with the left axis). In contrast to Europe, the change in the N criterion hardly matters in China. This is due to the fact, that S depositions are main driver of exceedances in China. The changes in critical pH result in a reduction/increase of the non-exceeded area of about 5 % (around a reference value of 50 %).

Discussion and concluding remarks

Combining databases on soil, land cover, climate and forest growth provided detailed maps with more than 3 million receptors for Europe and about 4 million receptors in China, suitable for spatially highly disaggregated critical load calculations, demonstrating that the critical loads methodology can be applied on a large regional scale in different parts of the globe yielding results for comparable assessments.

In applications to date, critical loads of acidity and eutrophication have been treated separately. However, the growing emphasis on biodiversity (especially plant diversity) renders the separation between acidifying and eutrophying effects inappropriate (especially with respect to N). Therefore we combined in this paper the two approaches into a common critical load function for N and S and computed them on large regional scales (China and Europe). In this exercise we have chosen pH and N concentration criteria without taking into account possible interdependencies between the two variables. However, when looking at the occurrence of plant species or species compositions, the influential abiotic factors, such as pH or [N], are not independent from each other (e.g. Wamelink et al. 2011). Vegetation models that link species occurrence with abiotic factors could be used to derive combined pH-N-limits for the derivation of critical load functions for plant diversity (for a discussion of the issues

involved when dealing with combined criteria of [N] and pH see Posch et al. (2011)). The strong dependence of the critical loads on precipitation shows the limitations of assuming a relationship between N concentration and plant species sensitivity, whereas N availability, or other less fluctuating N quantities, may be more appropriate (De Vries et al. 2010). It should also be mentioned that some authors link the *cumulative* deposition of N to changes in plant species diversity (e.g. Duprè et al. 2010), which would call for a re-formulation of the 'critical load' concept.

The overall uncertainty of the critical loads is determined by model uncertainty and parameter uncertainty (see, e.g., Zak and Beven 1999; Skeffington et al. 2007). Parameter uncertainty can be substantial and strongly contribute to uncertainty in critical loads (De Vries et al. 1994). Others have shown that different methods of estimating weathering rates can yield strongly varying results (Hodson and Langan 1999). Model structure is another important source of uncertainty. The SMB model is by design a very simple model of reality; and the simple denitrification sub-model and the assumption of a homogenous soil layer contribute to uncertainty. Also, previous studies have shown that there is a strong effect of the depth at which the chemical criterion should be met (De Vries et al. 1994).

Although the future N and S deposition scenario used in this paper is motivated by climate change goals, it leads to a strong reduction of present S deposition in Europe and Asia (70–80 %) by 2100. Also N deposition is reduced by about 50 % in Europe, but only by a small fraction in Asia. But as the exceedance calculations carried out in this paper show, only further reductions of (mostly N) emissions will achieve the long-term objective of non-exceedance of critical loads. We think that studies like this could also complement the work carried out by the Task Force on hemispheric transport of air pollution (HTAP) under the LRTAP Convention, which aims at improving the understanding of the intercontinental transport of air pollutants across the Northern Hemisphere.

Acknowledgments We thank Jean-Francois Lamarque and Frank Dentener for providing the deposition fields of S and N. MP's and GJR's work was partially funded by the European Union's FP7 project 'ECLAIRE' (grant agreement no. 282910). LD's and YZ's work was partially funded by the Natural Science Foundation of China (project numbers 21221004 and 41205110).

References

Aherne J, Farrell EP, Hall J, Reynolds B, Hornung M (2001) Using multiple chemical criteria for critical loads of acidity in maritime regions. Water Air Soil Pollut Focus 1:75–90

Alexeyev VA, Markov MV, Birdsey RA (2004) Statistical data on forest fund of Russia and changing of forest productivity in the second half of the XX-th century. Ministry of Natural Resources of the Russian Federation, St. Petersburg Research Institute of Forestry and St. Petersburg Forest Ecological Center

Bartholome E, Belward AS, Achard F, Bartalev S, Carmona-Moreno C, Eva H, Fritz S, Gregoire M, Mayaux P, Stibig HJ (2002) GLC 2000. Global Land Cover mapping for the year 2000. Project status Nov 2002 (No. EUR 20524 EN). European Commission, Joint Research Centre, Ispra

Bashkin VN, Kozlov MY, Priputina IV, Abramychev AY, Dedkova IS (1995) Calculationandmapping of critical loads of S, N and acidity on ecosystems of the Northern Asia. Water Air Soil Pollut 85:2395–2400

Belyazid S, Kurz D, Braun S, Sverdrup H, Rihm B, Hettelingh J-P (2011) A dynamic modelling approach for estimating critical loads of nitrogen based on plant community changes under a changing climate. Environ Pollut 159:789–801

Bobbink R, Hettelingh J-P (eds) (2011) Review and revision of empirical critical loads and dose-response relationships. Proceedings of an expert workshop, ISBN 978-90-6960-251-6, Bilthoven, The Netherlands

Bouwman A, Van Vuuren D, Derwent R, Posch M (2002) A global analysis of acidification and eutrophication of terrestrial ecosystems. Water Air Soil Pollut 141:349–382

Davies CE, Moss D, Hill MO (2004). EUNIS habitat classification revised 2004. European environment agency, European topic centre on nature protection and biodiversity; http://eunis.eea.europa.eu

De Vries W, Reinds GJ, Posch M (1994) Assessment of critical loads and their exceedance on European forests using a one-layer steady-state model. Water Air Soil Pollut 72:357–394

De Vries W, Posch M, Hewitt CN, Jackson AV (2003) Critical levels and critical loads as a tool for air quality management. In: Hewitt AV (ed) Handbook of atmospheric science—principles and applications. Blackwell Science, Oxford, pp 562–602

De Vries W, Wamelink GWW, Van Dobben H, Kros J, Reinds GJ, Mol-Dijkstra JP, Smart SM, Evans CD, Rowe EC, Belyazid S, Sverdrup HU, Van Hinsberg A, Posch M, Hettelingh J-P, Spranger T, Bobbink R (2010) Use of dynamic soil-vegetation models to assess impacts of nitrogen deposition on plant species composition: an overview. Ecol Appl 20:60–79

Duan L, Xie SD, Zhou ZP, Hao JM (2000) Critical loads of acid deposition on soil in China. Water Air Soil Pollut 118:35–51

Duan L, Hao JM, Xie SD, Zhou ZP, Ye XM (2002) Determining weathering rates of soils in China. Geoderma 110:205–225

Duan L, Huang YM, Hao JM, Xie SD, Hou M (2004) Vegetation uptake of nitrogen and base cations in China and its role in soil acidification. Sci Total Environ 330:187–198

Duan L, Lin Y, Zhu XY, Tang GG, Gao DF, Hao JM (2007) Modeling atmospheric transport and deposition of calcium in China. J Tsinghua Univ 47:1462–1465 (in Chinese)

Duprè C, Stevens CJ, Ranke T, Bleeker A, Peppler-Lisbach C, Gowing DJG, Dise NB, Dorland E, Bobbink R, Diekmann M (2010) Changes in species richness and composition in European acidic grasslands over the past 70 years: the contribution of cumulative atmospheric nitrogen deposition. Glob Change Biol 16:344–357

European Soil Bureau network (2004) European soil database (v 2.0) (No. EUR 19945 EN). European Soil Bureau Network and European Commission, Ispra

FAO-UNESCO (2003) Digital soil map of the world and derived soil properties, CD-ROM. FAO, Rome

Forsius M, Posch M, Aherne J, Reinds GJ, Christensen J, Hole L (2010) Assessing the impacts of long-range sulfur and nitrogen deposition on arctic and sub-arctic ecosystems. Ambio 39:136–147

Hao JM, Duan L, Zhou XL, Fu LX (2001) Application of a LRT model to acid rain control in China. Environ Sci Technol 35:3407–3415

Hao JM, Qi CL, Duan L, Zhou ZP (2003) Evaluating critical loads of nutrient nitrogen on soils in China using the SMB method. J Tsinghua Univ 43:849–853 (in Chinese)

Henriksen A, Kämäri J, Posch M, Wilander A (1992) Critical loads of acidity: nordic surface waters. Ambio 21:356–363

Hettelingh J-P, Sverdrup H, Zhao D (1995a) Deriving critical loads for Asia. Water Air Soil Pollut 85:2565–2570

Hettelingh J-P, Posch M, De Smet PAM, Downing RJ (1995b) The use of critical loads in emission reduction agreements in Europe. Water Air Soil Pollut 85:2381–2388

Hettelingh J-P, Posch M, De Smet PAM (2001) Multi-effect critical loads used in multi-pollutant reduction agreements in Europe. Water Air Soil Pollut 130:1133–1138

Hettelingh J-P, Posch M, Slootweg J, Reinds GJ, Spranger T, Tarrason L (2007) Critical loads and dynamic modelling to assess European areas at risk of acidification and eutrophication. Water Air Soil Pollut Focus 7:379–384

Hettelingh J-P, Posch M, Velders GJM, Ruyssenaars P, Adams M, De Leeuw F, Lükewille A, Maas R, Sliggers J, Slootweg J (2013) Assessing interim objectives for acidification, eutrophication and ground-level ozone of the EU National Emission Ceilings Directive with 2001 and 2012 knowledge. Atmos Environ 75:129–140

Hodson ME, Langan SJ (1999) Considerations of uncertainty in setting critical loads of acidity of soils: the role of weathering rate determination. Environ Pollut 106:73–81

ICP Modelling and Mapping (2004) Manual on methodologies and criteria for modelling and mapping critical loads & levels and air pollution effects, risks and trends. Texte 52/04, Federal Environmental Agency, Berlin, Germany [for latest updates see www.icpmapping.org

Jacobsen C, Rademacher P, Meesenburg H, Meiwes KJ (2002) Element contents in tree compartments—literature study and data collection [in German]. Niedersächsische Forstliche Versuchsanstalt, Göttingen, p 80

Jeffries DS, Lam DCL (1993) Assessment of the effect of acidic deposition on Canadian lakes: determination of critical loads for sulphate deposition. Water Sci Technol 28:183–187

JRC (2006) The European Soil Data Base. Distribution version v2.0. Retrieved 01-01-2007, http://eusoils.jrc.it/ESDB_Archive/ESDBv2/index.htm

Kuylenstierna JCI, Rodhe H, Cinderby S, Hicks K (2001) Acidification in developing countries: ecosystem sensitivity and the critical load approach on a global scale. Ambio 30:20–28

Lamarque J-F, Dentener F, McConnell J, Ro C-U, Shaw M, Vet R, Bergmann D, Cameron-Smith P, Dalsoren S, Doherty R, Faluvegi G, Ghan SJ, Josse B, Lee YH, MacKenzie IA, Plummer D, Shindell DT, Skeie RB, Stevenson DS, Strode S, Zeng G, Curran M, Dahl-Jensen D, Das S, Fritzsche D, Nolan M (2013) Multi-model mean nitrogen and sulfur deposition from the Atmospheric Chemistry and Climate Model Intercomparison Project (ACCMIP): evaluation of historical and projected future changes. Atmos Chem Phys 13:7997–8018

Lee DS, Pacyna JM (1999) An industrial emissions inventory of calcium for Europe. Atmos Environ 33:1687–1697

Leemans R, Van den Born GJ (1994) Determining the potential distribution of vegetation, crops and agricultural productivity. Water Air Soil Pollut 76:133–161

New M, Hulme M, Jones PD (1999) Representing twentieth century space-time climate variability. Part 1: development of a 1961–90 mean monthly terrestrial climatology. J Clim 12:829–856

Nilsson J, Grennfelt P (eds) (1988) Critical loads for sulphur and nitrogen: Miljørapport 15. Nordic Council of Ministers, Copenhagen

Pardo LH, Fenn ME, Goodale CL, Geiser LH, Driscoll CT, Allen EB, Baron JS, Bobbink R, Bowman WD, Clark CM, Emmett B, Gilliam FS, Greaver TL, Hall SJ, Lilleskov EA, Liu L, Lynch JA, Nadelhoffer KJ, Perakis SS, Robin-Abbott MJ, Stoddard JL, Weathers KC, Dennis RL (2011) Effects of nitrogen deposition and empirical nitrogen critical loads for ecoregions of the United States. Ecol Appl 21:3049–3082

Posch M, De Vries W (1999) Derivation of critical loads by steady-state and dynamic soil models. In: Langan SJ (ed) The impact of nitrogen deposition on natural and semi-natural ecosystems. Kluwer, Dordrecht, pp 213–234

Posch M, Hettelingh J-P, De Smet PAM (2001) Characterization of critical load exceedances in Europe. Water Air Soil Pollut 130:1139–1144

Posch M, Aherne J, Hettelingh J-P (2011) Nitrogen critical loads using biodiversity-related critical limits. Environ Pollut 159:2223–2227

Prentice IC, Sykes MT, Cramer W (1993) A simulation model for the transient effects of climate change on forest landscapes. Ecol Model 65:51–70

Reinds GJ, De Vries W (2010) Uncertainties in critical loads and target loads of sulphur and nitrogen for European forests: analysis and quantification. Sci Total Environ 408:1960–1970

Reinds GJ, Posch M, De Vries W, Slootweg J, Hettelingh J-P (2008) Critical loads of sulphur and nitrogen for terrestrial ecosystems in Europe and northern Asia using different soil chemical criteria. Water Air Soil Pollut 193:269–287

Reis S, Grennfelt P, Klimont Z, Amann M, ApSimon H, Hettelingh J-P, Holland M, Le Gall A-C, Maas R, Posch M, Spranger T, Sutton MA, Williams M (2012) From acid rain to climate change. Science 338:1153–1154

Schelhaas MJ, Varis S, Schuck A, Nabuurs GJ (1999) EFISCEN's european forest resource database. European Forest Institute, Joensuu

Schelhaas MJ, Eggers J, Lindner M, Nabuurs GJ, Pussinen A, Paivinen R, Schuck A, Verkerk PJ, Van der Werf DC (2007) Model documentation for the European Forest Information Scenario Model (EFISCEN 3.1.3). Alterra Report 1559, Wageningen, The Netherlands

SinoMaps (1984) Atlas of the People's Republic of China, 3rd ed (in Chinese). SinoMaps Press, Beijing

Skeffington RA, Whitehead PG, Heywood E, Hall JR, Wadsworth RA, Reynolds B (2007) Estimating uncertainty in terrestrial critical loads and their exceedances at four sites in the UK. Sci Total Environ 382:199–213

Sverdrup H, De Vries W (1994) Calculating critical loads for acidity with the simple mass balance method. Water Air Soil Pollut 72:143–162

Van Loon M, Tarrason L, Posch M (2005) Modelling base cations in Europe. EMEP Technical Report MSC-W 2/2005. Norwegian Meteorological Institute, Oslo

Van Vuuren DP, Edmonds J, Kainuma M, Riahi K, Thomson A, Hibbard K, Hurtt GC, Kram T, Krey V, Lamarque J-F, Masui T, Meinshausen M, Nakicenovic N, Smith SJ, Rose SK (2011) The representative concentration pathways: an overview. Clim Change 109:5–31

Wamelink GWW, Goedhart PW, Malinowska AH, Frissel JY, Wegman RJM, Slim PA, Van Dobben HF (2011) Ecological ranges for the pH and NO_3 of syntaxa: a new basis for the estimation of critical loads for acid and nitrogen deposition. J Veg Sci 22:741–749

Wu ZY (ed) (1980) Chinese Vegetation (in Chinese). Science Press, Beijing

Xiong Y, Li QK (eds) (1987). Chinese Soils, 2nd ed (in Chinese). Science Press, Beijing

Zak SK, Beven KJ (1999) Equifinality, sensitivity and predictive uncertainty in the estimation of critical loads. Sci Total Environ 236:191–214

Zhao Y, Duan L, Larssen T, Hu LH, Hao JM (2007) Simultaneous assessment of depositions of base cations, sulfur and nitrogen using an extended critical load function for acidification. Environ Sci Technol 41:1815–1820

Zhao Y, Duan L, Lei Y, Xing J, Nielsen CP, Hao JM (2011) Will PM control undermine China's efforts to reduce soil acidification? Environ Pollut 159:2726–2732

Zhu XY, Duan L, Tang GG, Hao JM, Dong GX (2004) Estimation of atmospheric emissions of base cations in China. J Tsinghua Univ 44:1176–1179 (in Chinese)